119 J. H. Shin, J. K. Paik, J. R. Price, and M. A. Abidi, "Adaptive regularized image interpolation using data fusion and steerable constraints," Proc. SPIE Visual Comm., Image Proc., Vol. 4310, pp. 798-809, San Jose, CA, January 2001.

Adaptive regularized image interpolation using data fusion and steerable constraints

Jeong-Ho Shin[a], Joon-Ki Paik[a], Jeffery R. Price[b], and Mongi A. Abidi[b]

[a]Department of Image Engineering,
Graduate School of Advanced Imaging Science, Multimedia, and Film, Chung-Ang University
221 Huksuk-Dong, Tongjak-Ku, Seoul 156-756, Korea
[b]Department of Electrical and Computer Engineering,
University of Tennessee, Knoxville, TN, USA

ABSTRACT

This paper presents an adaptive regularized image interpolation algorithm from blurred and noisy low resolution image sequence, which is developed in a general framework based on data fusion. This framework can preserve the high frequency components along the edge orientation in a restored high resolution image frame. This multiframe image interpolation algorithm is composed of two levels of fusion algorithm. One is to obtain enhanced low resolution images as an input data of the adaptive regularized image interpolation based on data fusion. The other one is to construct the adaptive fusion algorithm based on regularized image interpolation using steerable orientation analysis. In order to apply the regularization approach to the interpolation procedure, we first present an observation model of low resolution video formation system. Based on the observation model, we can have an interpolated image which minimizes both residual between the high resolution and the interpolated images with a prior constraints. In addition, by combining spatially adaptive constraints, directional high frequency components are preserved with efficiently suppressed noise. In the experimental results, interpolated images using the conventional algorithms are shown to compare the conventional algorithms with the proposed adaptive fusion based algorithm. Experimental results show that the proposed algorithm has the advantage of preserving directional high frequency components and suppressing undesirable artifacts such as noise.

Keywords: Image interpolation, data fusion, steerable filter, regularization, resolution enhancement, adaptive edge preserving

1. INTRODUCTION

High resolution (HR) restoration has many applications in image processing. There are two categories in high resolution restoration. One is the traditional image restoration concerned with the reconstruction of an uncorrupted image from a blurred and noisy one.[1] The other one is the image interpolation associated with increase of the spatial resolution of a single or a set of image frames.[2,3] HR image processing applications such as digital high-definition television (HDTV), aerial photo, medical imaging, surveillance video and military purpose images, need HR image interpolation algorithms.

In this paper, we mainly deal with image interpolation algorithms to enhance the image quality in the sense of resolution. By introducing image fusion and adaptive regularization algorithms, the proposed algorithm can restore HR image from low-resolution (LR) video. Originally, the objective of image fusion is to combine information from multiple images of the same scene. As a result of image fusion, a single image which is more suitable for human and machine perception or further image-processing tasks can be obtained.[4] Data fusion algorithms are usually used in applications ranging from Earth resource monitoring, weather forecasting, and vehicular traffic control to military target classification and tracking.[5] By utilizing the nature of image fusion mentioned above, we can not only make

Further author information: (Send correspondence to J. K. Paik)
J. H. Shin : E-mail: shinj@ms.cau.ac.kr
J. K. Paik : E-mail: paikj@cau.ac.kr
J. R. Price :E-mail: jrp@utk.edu
M. A. Abidi : E-mail: abidi@utk.edu

adequate LR image frames to higher resolution restoration, but also construct a general framework based on image fusion toward the problem of multiframe image interpolation.

Many algorithms have been proposed to improve the resolution of images. Conventional interpolation algorithms, such as zero-order or nearest neighbor, bilinear, cubic B-spline, and the DFT-based interpolation, can be classified by basis functions, and they focus on just enlargement of image.[2,6,7] Those algorithms have been developed under assumption that there are no mixture among adjacent pixels in the imaging sensor, no motion blur due to finite shutter speed of the camera, no isotropic blur due to out-of-focus, and no aliasing in the process of sub-sampling. Since the assumptions mentioned above are not satisfied in general low-resolution imaging systems, it is not easy to restore the original high-resolution image by using the conventional interpolation algorithms.

In order to improve the performance of the above mentioned algorithms, a spatially adaptive cubic interpolation method has been proposed in.[8] Although it can preserve a number of directional edges in the interpolation process, it is not easy to restore original high frequency components which are lost in the sub-sampling process. As a alternative, multi-frame interpolation techniques which use sub-pixel motion information have been proposed in.[9–25]

It is well-known that image interpolation is an ill-posed problem. More specifically, we regard a sub-sampling process as a general image degradation process. Then the regularized image interpolation is to find the inverse solution defined by the image degradation model subject to *a priori* constraint.[12,13] Since the conventional regularized interpolation methods used isotropic smoothness as a prior constraints, their interpolation performance for images with various edges is limited.

As another approach to the high-resolution image interpolation problem, Schultz and Stevenson have addressed a method for nonlinear single-channel image expansion which preserves the discontinuities of the original image based on the maximum a *posteriori* (MAP) estimation technique.[26] They also proposed a video superresolution algorithm, which used MAP estimator with edge preserving Huber-Markov random field (HMRF) prior.[14] A similar approach to the superresolution problem was suggested by Hardie, Barnard, and Amstrong, which simultaneously estimates image registration parameters and the high-resolution image.[16] However, all of these methods have similar Gibbs priors which represent non-adaptive smoothness constraints.

A spatial image interpolation algorithm using projections onto convex sets (POCS) theory, which obtains high resolution images from low resolution image sequences, has been studied in.[15,10,18,11,27,28] In general, POCS methods have a simple structure to implement, while theoretical and numerical shortcomings, such as non-uniqueness of solution and considerable computation, are included in these approaches. For regularized interpolated methods, deterministic or statistical information about the fidelity to high-resolution image and statistical information about the smoothness prior are incorporated to obtain the feasible solution between constraint sets. Therefore, regularization-based interpolation methods may provide more feasible estimates than POCS-based ones. On the other hand, a hybrid algorithm combining optimized method, such as the maximum likelihood (ML), MAP, and POCS approaches, was presented by Elad and Feuer.[19] They used the regularization weight matrix with locally adaptive smoothness to obtain higher resolution image quality. A multiframe interpolation algorithm for color video sequence is suggested by Shah and Zakhor.[21] They used a set of candidate motion estimates and chrominance components to compute accurate motion vectors. In,[29] modified edge-based line average (ELA) techniques for the scanning rate conversion is proposed. Nevertheless, all of the above estimated HR image may have no high frequency details along edges.

This paper proposes a general framework based on image fusion algorithm toward the problem of multi-frame image interpolation. Restored HR image frames with high frequency components along the direction of edges can be obtained from low resolution image frames. In this paper, data fusion approaches are applied to obtain enhanced HR images and used to analyze the structure of regularized image interpolation algorithms.

This paper is arranged as follows. Section 2 defines mathematical observation models of LR image formation system. In Section 3, we propose a general framework of multiframe image interpolation algorithm based on image fusion. Also, steerable filter-based orientation analysis algorithms and new constraints are presented in Section 3. Some experimental results for high resolution image interpolation are provided in Section 4. Finally, Section 5 concludes the paper.

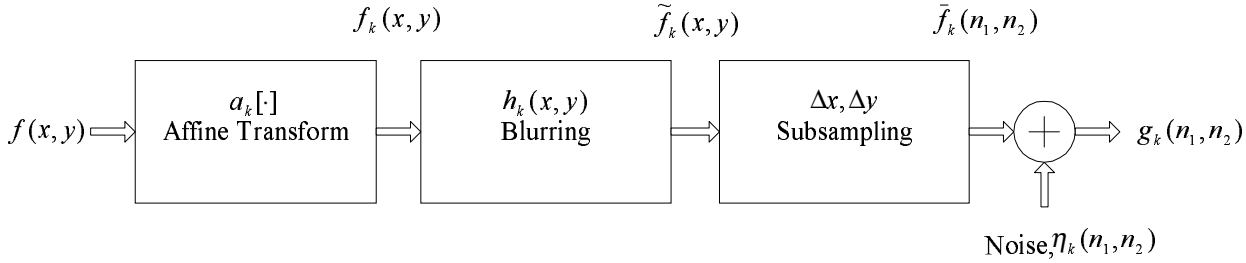

Figure 1. Observation model of LR video formation system.

2. OBSERVATION MODEL

In this section, we present an observation model of LR video formation system. Two models are presented: we first present a model that relates the LR sampled video to the HR continuous image. Then the discrete-discrete model is followed.

2.1. Continuous-discrete model

Assume that a three-dimensional (3D) object or scene has been imaged onto a two-dimensional (2D) imaging plane. A block diagram of the observation model is shown in Fig. 1. The original input HR image is denoted by $f(x,y)$ in the continuous 2D coordinate system (x,y). Here we assume that the HR image goes through several degradation aspects such as an affine transform, blurring, and subsampling process. First, an affine transformation including three basic transformations as translation, scaling, and rotation, are modeled to give a motion in the original HR image. According to the model, the k-th observed image frame in a sequence can be expressed as

$$f_k(x,y) = a_k[f(x,y)]_{\mathbf{d}_k,\theta_k,\mathbf{s}_k}, \quad \text{for} \quad k = 1,2,\cdots,L, \tag{1}$$

where a_k represents an affine transformation vector function with parameters, $\mathbf{d}_k, \theta_k, \mathbf{s}_k$ in the kth frame. Here $\mathbf{d}_k$ denotes a translation vector whose elements $\{d_x, d_y\}$, θ_k denotes a rotation angle, and $\mathbf{s}_k$ denotes two scaling factors, $\{s_x, s_y\}$.

The blurring effect of LR photo-detectors is modeled in the second step of the Fig. 1 by a convolution with the blur kernel, $h_k(x,y)$ as in

$$\tilde{f}_k(x,y) = f_k(x,y) ** h_k(x,y), \tag{2}$$

where $**$ represents a 2D convolution. Note that the blur is assumed to be spatially linear space-invariant (LSI) and temporally linear space-variant (LSV) in (2). In fact, the blurring effect of general image degradation system results from optical blurs such as out-of-focus blur as well as sensor blurs by limitation of the LR photo-detectors mentioned above. In order to simplify the observation model in this paper, however, we consider only the sensor blurs in the step of blurring. The third step of the observation model is subsampling with constant sampling intervals, $\Delta x, \Delta y$, on 2D rectangular sampling grid. Therefore, the subsampled version of $\tilde{f}_k(x,y)$ in (2) can be obtained as

$$\bar{f}_k(n_1,n_2) = \sum_{n_1=1}^{N_1} \sum_{n_2=1}^{N_2} \tilde{f}_k(x,y)\delta(x - n_1\Delta x, y - n_2\Delta y), \tag{3}$$

where δ represents the Dirac delta function.

Finally, the affine transformed, blurred, and subsampled discrete images, $\bar{f}_k(n_1,n_2)$ are corrupted by noise as

$$g_k(n_1,n_2) = \bar{f}_k(n_1,n_2) + \eta_k(n_1,n_2), \quad \text{for} \quad n_1 = 1,2,\cdots,N_1, \; n_2 = 1,2,\cdots,N_2. \tag{4}$$

The noise contribution is shown as an additive random process which is statistically uncorrelated with the image.

2.2. Discrete-discrete model

Now, the LR sampled image frames are expressed in terms of a HR sampled image. The HR restoration problem is then posed as the reconstruction of this HR image from a number of observed LR image frames. Let's assume that the HR continuous image, $f(x, y)$, is sampled over Nyquist rate, so that the sampled version of HR continuous image has no aliasing. By the ideal sampling with Nyquist rate, the discrete HR image, $f(m_1, m_2)$, can be produced. Here let the size of discrete HR image be $M_1 \times M_2$.

As the previous section, the discrete HR image goes through the same degradation steps as in Fig. 1. Of course, the function with continuous arguments f_k, g_k, h_k, and, η_k are replaced by arrays of samples taken on 2D rectangular grid. The first step for affine transformation yields the discrete image performing translation, scaling, and rotation from the discrete HR image, $f(m_1, m_2)$, as given in

$$f_k(m_1, m_2) = A_k[f(m_1, m_2)]_{\mathbf{d}_k, \theta_k, \mathbf{s}_k}, \quad \text{for} \quad m_1 = 1, 2, \cdots, M_1, \; m_2 = 1, 2, \cdots, M_2, \; k = 1, 2, \cdots, L. \tag{5}$$

Then, in order to account for the blurring effect of LR photo-detectors, the discrete blur function i.e. point spread function (PSF) is modeled and convolved with $f_k(m_1, m_2)$ in (5) as

$$\tilde{f}_k(m_1, m_2) = f_k(m_1, m_2) ** h_k(m_1, m_2). \tag{6}$$

Next, the affine transformed and blurred image is subsampled as

$$\bar{f}_k(n_1, n_2) = \tilde{f}_k(n_1 \frac{M_1}{N_1}, n_2 \frac{M_2}{N_2}), \quad \text{for} \quad n_1 = 1, 2, \cdots, N_1, \; n_2 = 1, 2, \cdots, N_2, \; k = 1, 2, \cdots, L. \tag{7}$$

Finally, the subsampled discrete images over Nyquist rate, $\bar{f}_k(n_1, n_2)$ are corrupted by noise as

$$g_k(n_1, n_2) = \bar{f}_k(n_1, n_2) + \eta_k(n_1, n_2). \tag{8}$$

As a result, L observed LR image frames, $\{g_k(n_1, n_2)\}_{k=1}^{L}$, can be obtained.

For simplification it is convenient to use the matrix-vector notation

$$g_k = H_k x + \eta_k, \quad \text{for} \quad k = 1, 2, \cdots, L. \tag{9}$$

where $H_k = S_k L_k A_k$. Here A_k denotes the $M^2 \times M^2$ affine transformation matrix for the HR image x of size $N^2 \times 1$, L_k is the blurring operator of size $M^2 \times M^2$, and S_k is the subsampling matrix of size $N^2 \times M^2$. Also, g_k and η_k respectively represent an additive Gaussian noise sample and the k-th observed LR image of size $N^2 \times 1$. To apply the data fusion algorithm in this paper, the observed LR image g_k in (9) is assumed to be the sensor image from the k-th imperfect LR sensor.

3. MULTIFRAME REGULARIZED IMAGE INTERPOLATION ALGORITHM

In this section, we propose a framework of multiframe image interpolation using data fusion and steerable constraints. The presented interpolation algorithm is introduced by the functional model as shown in Fig. 2. As shown in Fig. 2, this multiframe image interpolation algorithm is composed of two levels of fusion algorithm. In level-1 fusion, sensor data i.e. LR image sequence from LR imaging sensor is acquired and combined to obtain LR image frames with more information. Here, data from different sensors, or sensor channels within a common sensor, are combined before much preprocessing is performed.

Next, level-2 fusion processing fuses data compatibility and spatially adaptive smoothness constraints to regularize the ill-posed problem of image interpolation. Specially, this level processing performs mixing or voting images for the customized purpose. In this research, level-2 fuison is used to incorporate a spatially adaptive regularization algorithm, which restore/interpolate the HR image from blurred and noisy LR image frames by mixing or voting the pixel which is suitable for human visual system. As a result, the HR image is restored from several LR sensor images.

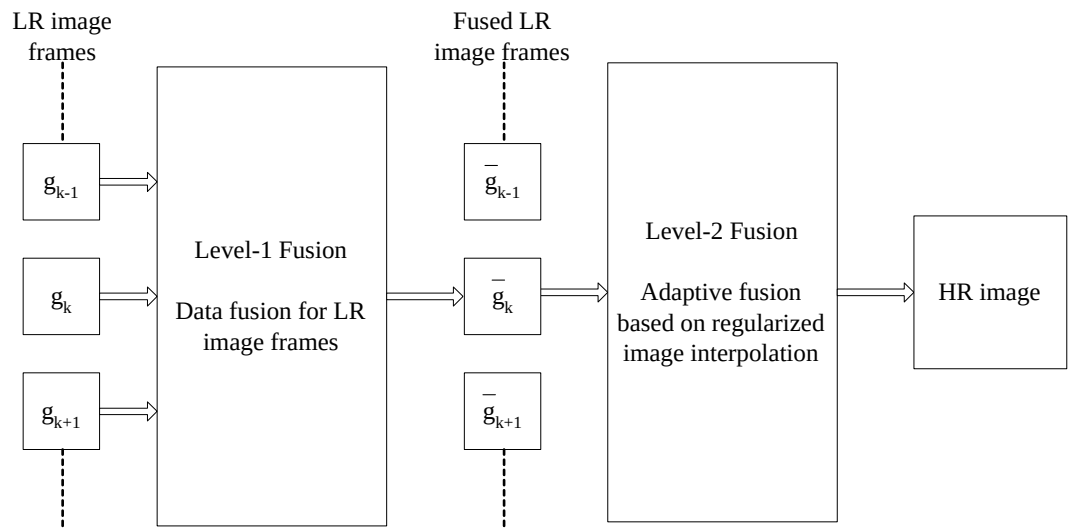

Figure 2. The structure of the proposed multiframe image interpolation.

3.1. Data fusion for LR image frames: Level-1 fusion

A brief review of the data fusion algorithm, which combines two or more LR image frames to provide more feasible input image, is presented in this section. In order to perform this level-1 fusion, sensor data is registered by data alignment processing. Although the purpose of this research is image interpolation with respect to the same scene, the image frames from single sensor may include arbitrary motion due to moving objects. Therefore, data alignment is performed through spatial and temporal reference adjustments and coordinate system selection and transformations that establish a common space-time reference for fusion processing.[5] Further details are provided in previous works.[24,25] Data fusion can be implemented at either the signal, the pixel, the feature or the symbolic level of representation. Here, we use pixel-level fusion which is to merge multiple images on pixel-by-pixel basis to improve the performance of many image processing tasks.[30,4] The reason why we use fusion concept in this algorithm is that it has advantages for image interpolation. As mentioned before, it presents a better resolution and information of the scene than the one obtained using only one data set.

There are two approaches to combine LR image frames in the sense of processing domain. One is spatial domain processing using a gradient and local variance,[24] and the other is the transformed domain processing using discrete wavelet transforms (DWT), discrete wavelet frame (DWF),[25] and steerable pyramid, etc. By performing the level-1 fusion in the section, fused LR image frames can be constructed as $\{\bar{g}_k(n_1, n_2)\}_{k=1}^{L}$. After the data fusion process of this section, we perform the adaptive fusion based on regularized image interpolation algorithm presented in Sec. 3.2.

3.2. Adaptive fusion based on regularized image interpolation: Level-2 fusion

This level-2 fusion incorporates a voting fusion into the existing iterative regularization structure which fuses data compatibility and smoothness of the solution to solve the ill-posed problem. However, the existing regularized image interpolation algorithms do not satisfy the human visual system.[23] The human visual characteristics are partly revealed by psychophysical experiments. According to those experiments, human visual system is sensitive to noise in flat regions, while it becomes less sensitive to noise at sharp transitions in image intensity. In conclusion, human visual system is less sensitive to noise in edges than in flat regions.[31] Based on the results of the experiments, various ways to subjectively improve the quality of the restored image have been proposed in.[32,33] In this section, we introduce new adaptive fusion algorithm which is adequate to human visual system and present its efficient implementation. Also, the steerable orientation analysis and its spatially adaptive constraints are presented to apply the adaptive voting fusion algorithm as a criterion of feature classification.

3.2.1. The existing regularization approach

In order to solve (9), the regularized image interpolation algorithm tries to find the estimate, $\hat{x}$, which satisfies the following optimization problem.[22]

$$\hat{x} = \overset{\arg\min}{x} f(x), \tag{10}$$

where

$$f(x) = \sum_{k=1}^{L} f_k(x) = \sum_{k=1}^{L} \left[||\bar{g}_k - H_k x||^2 + \lambda ||Cx||^2 \right], \tag{11}$$

where C is a $M^2 \times M^2$ matrix which represents a high-pass filter, and $||Cx||^2$ represents a stabilizing functional whose minimization suppresses high frequency components due to noise amplification. And λ represents the regularization parameter which controls the fidelity to the original image, $||\bar{g}_k - H_k x||^2$, and smoothness of the restored image, $||Cx||^2$.

The cost function given in (11) can be minimized as[34]

$$\sum_{k=1}^{L} [H_k^T H_k + \lambda C^T C] x = \sum_{k=1}^{L} H_k^T \bar{g}_k. \tag{12}$$

The above solution in (12) results from a batch processing which assumes that all data are available to be considered simultaneously. That is, we assume that all n observations are available, select an optimization criterion, and proceed to find the value of x that best fits the L observations. Batch approach is often used in situations for which no time critical element is involved. These approaches have an advantage of getting more feasible solutions.

In order to solve the above equation given in (12), the successive approximation equation describing the interpolated image x, at the $(l+1)$-th iteration step, is given by

$$x^{l+1} = x^l + \beta \{ \sum_{k=1}^{L} H_k^T \bar{g}_k - \sum_{k=1}^{L} [H_k^T H_k + \lambda C^T C] x^l \} \tag{13}$$

where $\bar{g}_k$ represents the fused LR image frame from P consecutive LR image frames $\{g_{k-\frac{P-1}{2}}, \cdots, g_k, \cdots, g_{k+\frac{P-1}{2}}\}$, with odd P, and β the relaxation parameter that controls the convergence as well as convergence rate. In dealing with iterative algorithms, the convergence and the rate of convergence are very important. Unless convergence is guaranteed, the iterative algorithm cannot be used. Even if convergence is guaranteed, sufficiently high rate of the convergence is needed for practical applications. In-depth convergence analysis has been proposed in.[33]

3.2.2. Steerable filter based orientation analysis[35]

This section provides an orientation analysis algorithm to apply the adaptive image fusion using regularization in next section. Oriented filters are useful in many image processing and early vision tasks. Freeman and Adelson developed the concept of steerable filters, in which a filter of arbitrary orientation is synthesized as a linear combination of a set of basis filters. The quadrature pair filters are the derivative Gaussian filters and their Hilbert transform respectively. The basic idea of steerable filters is to apply the a small number oriented basis filters to an image and then, by linear combination of the responses to the different filters, determines the responses of filter oriented in an arbitrary direction.

In this paper, two different sets of steerable filters are used resulting in: a steered filter corresponding to the second derivative of a Gaussian filter. For a Gaussian filter, the following basis filters are used.

$$\begin{aligned} G_{2a} &= 0.92132(2{x^2}_1 - 1)e^{-(x^2+y^2)} \\ G_{2b} &= 1.84264xye^{-(x^2+y^2)} \\ G_{2c} &= 0.92132(2y^2 - 1)e^{-(x^2+y^2)}. \end{aligned} \tag{14}$$

The corresponding steering functions are :

$$\begin{aligned} K_a(\theta) &= \cos^2(\theta) \\ K_b(\theta) &= -2\cos(\theta)\sin(\theta) \\ K_c(\theta) &= \sin^2(\theta). \end{aligned} \tag{15}$$

A synthesized filter oriented along any direction θ can be represented as:

$$G_2^\theta = (K_a(\theta)G_{2a} + K_b(\theta)G_{2b} + K_c(\theta)G_{2c}). \tag{16}$$

A quadrature pair is formed using a Hilbert transformation of the Gaussian filters. A normalized numerical approximation of the Hilbert transform was obtained, resulting in the following four basis filters:

$$\begin{aligned} H_{2a} &= 0.97780(-2.254x + y^3)e^{-(x^2{}_1+y^2)} \\ H_{2b} &= 0.97780(-0.7515 + x^2)ye^{-(x^2+y^2)} \\ H_{2c} &= 0.97780(-0.7515 + y^2)xe^{-(x^2+y^2)} \\ H_{2d} &= 0.97780(-2.254y + y^3)e^{-(x^2+y^2)}. \end{aligned} \tag{17}$$

The corresponding steering function are:

$$\begin{aligned} K_a(\theta) &= \cos^3(\theta) \\ K_b(\theta) &= -3\cos^2(\theta)\sin(\theta) \\ K_c(\theta) &= 3\cos(\theta)\sin^2(\theta) \\ K_d(\theta) &= -\sin^3(\theta). \end{aligned} \tag{18}$$

The resulting filter steered in the direction θ is

$$H_2^\theta = (K_a(\theta)H_{2a} + K_b(\theta)H_{2b} + K_c(\theta)H_{2c} + K_d(\theta)H_{2b}). \tag{19}$$

Using the nth derivative of a Gaussian and its Hilbert transform as our bandpass filters, we have

$$E_n(\theta) = [G_n^\theta]^2 + [H_n^\theta]^2. \tag{20}$$

Expressing the steered filter response in terms of the basis filters and steering weights reveals that the above energy estimate can be expressed as

$$\begin{aligned} E_n(\theta) &= C_1 + C_2\cos(2\theta) + c_3\cos(2\theta) \\ &+ \text{ higher order terms.} \end{aligned} \tag{21}$$

The dominant orientation (one that maximizes the output energy), θ_d, is given by

$$\theta_d = \frac{arg[C_2, C_3]}{2}. \tag{22}$$

and the orientation strength is

$$S_\theta = \sqrt{C_2^2 + C_3^2}. \tag{23}$$

3.2.3. Spatially adaptive image fuison using regularizaiton

As an alternative to the nonadaptive processing in (13), we propose a spatially adaptive fusion algorithm by using a set of P different high-pass filters, C_i, for $i = 1, \cdots, P$, to selectively suppress the high frequency component along the corresponding edge direction. We assume that the number of edge direction is defined as $P = 5$, and then each pixel in an image can be classified into one of monotone, horizontal edge, vertical edge, and two diagonal edges by steerable orientation analysis. By applying this adaptive fusion algorithm, the HR image can be interpolated from LR image frames, and five directional edges are preserved in the HR image, simultaneously.

To apply the proposed spatially adaptive fusion algorithm into the existing regularization, a isotropic high-pass filter C in (13) is replaced by a set of P different high-pass filters, C_i, for $i = 1, \cdots, P$, and the $(l+1)$-st regularized iteration step can be given as

$$x^{l+1} = x^l + \beta\{\sum_{k=1}^{L} H_k^T \bar{g}_k - [\sum_{k=1}^{L} H_k^T H_k + \sum_{i=1}^{P} \lambda_i I_i C_i^T C_i]x^l\}, \tag{24}$$

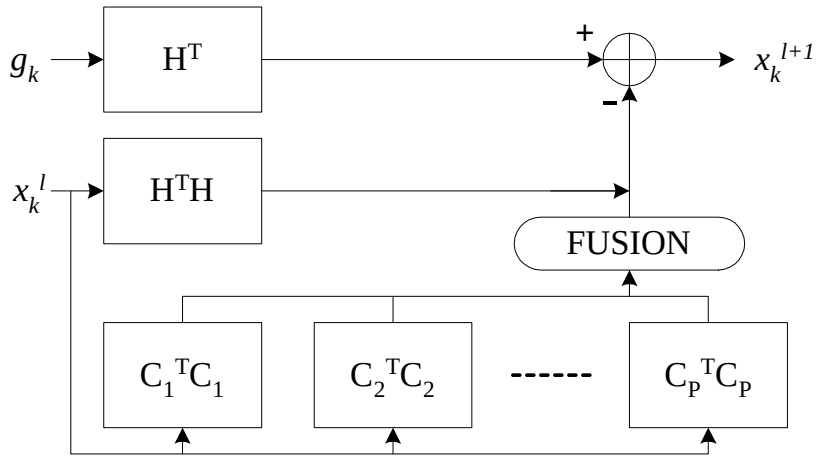

Figure 3. Adaptive fusion processing based on regularization.

where I_j represents a diagonal matrix with diagonal elements either zero or one. The properties of I_i can simply be summarized as

$$I_i I_j = 0, \text{ for } i \neq j, \text{ and } \sum_{i=1}^{M} I_i = I, \tag{25}$$

where I represents an $N^2 \times 1$ identity matrix. More specifically, diagonal element in I_j, which has one-to-one correspondence with each pixel in the image, is equal to one if it is on the corresponding edge, or zero otherwise.

In order to apply adaptive smoothness constraints to this algorithm, we should determine and classify the edge orientation in every pixels. At the same time, we should define spatially adaptive high-pass filters $\{C_i\}_{i=1}^{P}$, corresponding with the direction of dominant orientation at each pixel. In this paper, we use the steerable filter-based orientation analysis algorithm as an edge orientation classification algorithm in Sec. 3.2.2. Also, the corresponding directional constraints $C_i$can be defined as

$$C_1 = \frac{1}{16}\begin{bmatrix} 0 & 0 & -1 & 0 & 0 \\ 0 & -1 & -2 & -1 & 0 \\ -1 & -2 & 6 & -2 & -1 \\ 0 & -1 & -2 & -1 & 0 \\ 0 & 0 & -1 & 0 & 0 \end{bmatrix}, C_2 = \frac{1}{6}\begin{bmatrix} 0 & 0 & 0 & 0 & 0 \\ 0 & -1 & 2 & -1 & 0 \\ 0 & -1 & 2 & -1 & 0 \\ 0 & -1 & 2 & -1 & 0 \\ 0 & 0 & 0 & 0 & 0 \end{bmatrix}, C_3 = \frac{1}{6}\begin{bmatrix} 0 & 0 & 0 & 0 & 0 \\ 0 & -1 & -1 & -1 & 0 \\ 0 & 2 & 2 & 2 & 0 \\ 0 & -1 & -1 & -1 & 0 \\ 0 & 0 & 0 & 0 & 0 \end{bmatrix},$$

$$C_4 = \frac{1}{6}\begin{bmatrix} 0 & 0 & 0 & 0 & 0 \\ -1 & 2 & -1 & 0 & 0 \\ 0 & -1 & 2 & -1 & 0 \\ 0 & 0 & -1 & 2 & -1 \\ 0 & 0 & 0 & 0 & 0 \end{bmatrix}, C_5 = \frac{1}{6}\begin{bmatrix} 0 & 0 & 0 & 0 & 0 \\ 0 & 0 & -1 & 2 & -1 \\ 0 & -1 & 2 & -1 & 0 \\ -1 & 2 & -1 & 0 & 0 \\ 0 & 0 & 0 & 0 & 0 \end{bmatrix}. \tag{26}$$

The orientation analysis algorithm using steerable filter determines the direction, θ_d, and magnitude, S_θ, of dominant orientation at each pixel as given in (22) and (23). According to the direction of dominant orientation at each pixel, the current image x^l, is convolved with the corresponding high-pass filter C_i in (20). As a result, we can fuse directional smoothness constraints which act on preserving edges. Fig. 3 gives an overview of the proposed adaptive fusion processing based on regularization.

4. EXPERIMENTAL RESULTS

In order to demonstrate the performance of the proposed algorithm, we first make sixteen 64×64 LR image frames with white Gaussian noise of 20dB from the 256×256 HR lena image. In this experiment, we assume that the LR

(a) Original image (b) Ssubsampled image

Figure 4. Original image and synthetically subsampled image by factor of $\frac{1}{4}$ with 20[dB] additive Gaussian noise

image frames have global motion, 4×4 uniform blur, and subsampling process. Therefore, A_k has only translational motion components.

Fig. 4(a) represents the 256×256 HR lena image, 4(b) represents the sixteen 64×64 degraded images of (a) by using the degradation model in Sec. 2. Figs. 5(a) and 5(b) show the four times interpolated image of the first frame by using zero order interpolation method and by using bilinear interpolation method, respectively.

Figs. 6(a), and 6(b) respectively show interpolated images by using the existing regularized interpolation algorithm. For both interpolated images, iteration terminates after 10 iterations. Reguarization parameters λ, are respectively 0.01 and 1.0. As shown in Figs. 6(a)(b), large λ can suppress noise effectively but makes the image blurry in high frequency region. On the contrary, small λ in Fig. 6(b) makes noise amplified.

In Fig. 7(a), interpolated images by using the adaptive fusion algorithm excluding level-1 fusion is provided. Finally, we present the interpolated image by the proposed adaptive regularized interpolation algorithms using level-1 fusion, shown in Fig. 7(b). For both interpolated images, iteration terminates after 10 iterations and adaptive constraint sets in (26) are used. We can see some noise included in the image of Fig. 7(b) because of level-1 fusion. Actually, when level-1 fusion combines higher frequency components from severely noisy LR image frames, noise is also considered as high frequency components.

5. CONCLUSIONS

In this paper we proposed a general framework of multichannel image interpolation using data fusion and steerable filter. The proposed framework is composed of level 1, and 2. Level-1 fusion processing is performed in pixel level, and provides enhanced LR images so that HR image frames can be obtained in the main processing of level-2 fusion. Level-2 fusion is implemented in feature level. The features of this level provide the spatially adaptive constraints in the process of fusion. For example, edges of the LR image, i.e. features are classified and fused with data compatibility which can restore high resolution images. As a result, the fused image by level-2 fusion processing exists in the intersection of two uncertainty sets such as data compatibility set and smoothness constraint sets. For example, space variant regularization parameters λ_i, can be adopted in this level. In this paper, steerable constraints along the orientation of edge are used in level-2 processing.

In addition, the framework gives a generality multichannel image interpolation algorithms, that is, the conventional multi-channel interpolation algorithms can be analyzed by this framework using data fusion approach. The

(a) Zero-order interpolated image (PSNR=23.10[dB])

(b) Bilinear interpolated image (PSNR=21.46[dB])

Figure 5. Interpolation by the conventional algorithms

(a) Nonadaptive regularized interpolated image (PSNR=25.66[dB], $\lambda = 0.01$)

(b) Nonadaptively regularized interpolated image (PSNR=25.31[dB], $\lambda = 1.0$)

Figure 6. Interpolation by the existing regularization

(a) Adaptively regularized interpolated image (PSNR=25.60[dB], $\lambda_1 = 1.0, \lambda_{2-5} = 0.1$)

(b) Adaptively regularized interpolated image using level-1 fusion (PSNR=25.63[dB], $\lambda = 1.5, \lambda_{2-5} = 0.5$)

Figure 7. Interpolation by the proposed algorithms

algorithm can be divided into adaptive and non-adaptive version. The adaptive algorithm provides higher quality than non-adaptive version in the sense of high frequency details along the direction of edges.

The proposed framework presents the optimal solution to HR video with edge preserving constraints from LR video. By applying data fusion concept into this algorithm, regularized image interpolation algorithm, orientation analysis using steerable filter are combined in this framework.

ACKNOWLEDGMENTS

This research was supported in part by the Brain Korea 21 Project and in part by the University Research Program in Robotics under the United States Department of Energy, DOE-DE-FG02-86NE37968.

REFERENCES

1. H. C. Andrew and B. R. Hunt, *Digital Image Restoration*, Prentice-Hall, 1977.
2. A. K. Jain, *Fundamentals of Digital Image Processing*, Prentice-Hall, 1989.
3. J. S. Lim, *Two-Dimensional Signal and Image Processing*, Prentice-Hall, 1990.
4. Z. Zhang and R. C. Blum, "A categorization of multiscale-decomposition-based image fusion schemes with a performance study for a digital camera application," *Proc. IEEE* **87**, pp. 1315–1326, August 1999.
5. L. A. Klein, *Sensor and Data Fusion Concepts and Applications*, SPIE Optical Engineering Press, 1999.
6. M. Unser, A. Aldroubi, and M. Eden, "Fast b-spline transforms for continuous image representation and interpolation," *IEEE Trans. Pattern Analysis, Machine Intelligence* **13**, pp. 277–285, March 1991.
7. J. A. Parker, R. V. Kenyon, and D. E. Troxel, "Comparison of interpolating methods for image resampling," *IEEE Trans. Med. Imaging* **2**, pp. 31–39, March 1983.
8. K. P. Hong, J. K. Paik, H. J. Kim, and C. H. Lee, "An edge-preserving image interpolation system for a digital camcoder," *IEEE Trans. Consumer Electronics* **42**, pp. 279–284, August 1996.
9. S. P. Kim, H. K. Bose, and H. M. Valenzuela, "Recursive reconstruction of high-resolution image from noisy undersampled frames," *IEEE Trans. Acoust., Speech, Signal Processing* **38**, pp. 1013–1027, June 1990.

10. A. Patti, M. I. Sezan, and A. M. Tekalp, "High-resolution image reconstruction from a low-resolution image sequence in the presence of time varying motion blur," *Proc. 1994 Int. Conf. Image Processing* , November 1994.
11. A. Patti, M. I. Sezan, and A. M. Tekalp, "Superresolution video reconstruction with arbitrary sampling lattices and nonzero aperture time," *IEEE Trans. Image Processing* **6**, pp. 1064–1076, August 1997.
12. M. C. Hong, M. G. Kang, and A. K. Katsaggelos, "An iterative weighted regularized algorithm for improving the resolution of video sequences," *Proc. 1997 Int. Conf. Image Processing* **2**, pp. 474–477, October 1997.
13. B. C. Tom and A. K. Katsaggelos, "An iterative algorithm for improving the resolution of video sequences," *Proc, SPIE Visual Comm., Image Proc.* , pp. 1430–1438, March 1996.
14. R. R. Schultz and R. L. Stevenson, "Extraction of high-resolution frames form video sequences," *IEEE Trans. Image Processing* **5**, pp. 996–1011, June 1996.
15. J. H. Shin, J. H. Jung, and J. K. Paik, "Spatial interpolation of image sequences using truncated projections onto convex sets," *IEICE Trans. Fundamentals of Electronics, Communications, Computer Sciences* , June 1999.
16. R. C. Hardie, K. J. Barnard, and E. E. Armstrong, "Joint map registration and high-resolution image estimation using a sequence of undersampled images," *IEEE Trans. Image Processing* **6**, pp. 1621–1633, December 1997.
17. R. C. Hardie, K. J. Barnard, J. G. Bognar, E. E. Armstrong, and E. A. Watson, "High-resolution image reconstruction from a sequence of rotate and translated frames and its application to an infrared imaging system," *Optical Engineering* **37**, pp. 247–260, January 1998.
18. A. J. Patti, M. I. Sezan, and A. M. Tekalp, "High-resolution standards conversion of low resolution video," *Proc. 1995 Int. Conf. Acoust., Speech, Signal Processing* , pp. 2197–2200, 1995.
19. M. Elad and A. Feuer, "Restoration of a single superresolution image from several blurred, noisy, and undersampled measured images," *IEEE Trans. Image Processing* **6**, pp. 1646–1658, December 1997.
20. A. M. Tekalp, *Digital video processing*, Prentice-Hall, 1995.
21. N. R. Shah and A. Zakhor, "Resolution enhancement of color video sequences," *IEEE Trans. Image Processing* **8**, pp. 879–885, June 1999.
22. M. G. Kang and A. K. Katsaggelos, "Simultaneous multichannel image restoration and estimation of the regularization parameters," *IEEE Trans. Image Processing* **6**, pp. 774–778, May 1997.
23. J. H. Shin, J. H. Jung, and J. K. Paik, "Regularized iterative image interpolation and its application to spatially scalable coding," *IEEE Trans. Consumer Electronics* **44**, pp. 1042–1047, August 1998.
24. J. H. Shin, J. S. Yoon, and J. K. Paik, "Image fusion-based adaptive regularization for image expansion," *Proc. SPIE Image, Video Comm, Proc.* **3974**, pp. 1040–1051, January 2000.
25. J. H. Shin, J. H. Jung, J. K. Paik, and M. A. Abidi, "Adaptive image sequence resolution enhancement using multiscale decomposition based image fusion," *Proc, SPIE Visual Comm., Image Proc.* **3**, pp. 1589–1600, June 2000.
26. R. R. Schultz and R. L. Stevenson, "A bayesian approach to image expansion for improved definition," *IEEE Trans. Image Processing* **3**, pp. 233–242, May 1994.
27. H. J. Trussell and M. R. Civanlar, "The feasible solution in signal restoration," *IEEE Trans. Acoust. Speech Signal Processing* **ASSP-32**, pp. 201–212, April 1984.
28. D. C. Youla and H. Webb, "Image restoration by the method of convex projections: Part 1-theory," *IEEE Trans. Medical Imaging* **MI-1**, pp. 81–94, October 1982.
29. C. J. Kuo, C. Liao, and C. C. Lin, "Adaptive interpolation technique for scanning rate conversion," *IEEE Trans. Circuit, System, Video Technology* **6**, pp. 317–321, June 1996.
30. D. L. Hall, *Mathematical Techniques in Multisensor Data Fusion*, Artech House, 1992.
31. G. L. Anderson and A. N. Netravali, "Image restoration based on a subjective criterion," *IEEE Trans. Sys., Man, Cybern.* **SMC-6**, pp. 845–853, December 1976.
32. A. K. Katsaggelos, "Iterative image restoration algorithms," *Optical Engineering* **28**, pp. 735–748, 1989.
33. A. K. Katsaggelos, J. Biemond, R. W. Schafer, and R. M. Mersereau, "A regularized iterative image restoration algorithms," *IEEE Trans. Signal Processing* **39**(4), pp. 914–929, 1991.
34. N. P. Galatsanos, A. K. Katsaggelos, R. T. Chin, and A. D. Hillery, "Least square restoration of multichannel images," *IEEE Trans. Signal Processing* **39**, pp. 2222–2236, October 1991.
35. W. T. Freeman and E. H. Adelson, "The design and use of steerable filters," *IEEE Trans. Pattern Analysis, Machine Intelligence* **13**, pp. 891–906, September 1991.